

## Modeling the potential impact of climate change in northern Mexico using two environmental indicators

A. LÓPEZ SANTOS

*Unidad Regional Universitaria de Zonas Áridas, Universidad Autónoma Chapingo, Apartado Postal 8, 35230 Bermejillo, Durango, México*

*Miembro de la Red Temática del Agua del CONACyT*

Corresponding author; e-mail: alopez@chapingo.uruza.edu.mx

J. PINTO ESPINOZA

*Instituto Tecnológico de Durango, Blvd. Felipe Pescador 1830 Ote., Col. Nueva Vizcaya, 34080 Durango, Durango, México*

E. M. RAMÍREZ LÓPEZ

*Universidad Autónoma de Aguascalientes, Av. Universidad 940, Ciudad Universitaria, 20131 Aguascalientes, Aguascalientes, México*

M. A. MARTÍNEZ PRADO

*Instituto Tecnológico de Durango, Blvd. Felipe Pescador 1830 Ote., Col. Nueva Vizcaya, 34080 Durango, Durango, México*

Received June 4, 2012; accepted May 28, 2013

### RESUMEN

La modelación de impactos locales, caracterizados por deterioro de los recursos naturales –especialmente agua y suelo– ante los efectos globales del cambio climático, se ha convertido en una poderosa herramienta en la búsqueda de medidas de mitigación y adaptación. Los objetivos de la presente investigación fueron: 1) evaluar mediante procesos de modelación el impacto potencial del cambio climático para el periodo 2010-2039 y 2) advertir sobre riesgos futuros a partir de la identificación de forzantes radiativos locales o áreas críticas, considerando el índice de aridez (IA) y erosión laminar del suelo causada por el viento (ELV) como dos indicadores de calidad ambiental. Se usaron técnicas de evaluación de los recursos naturales empleadas por el Instituto Nacional de Ecología y Cambio Climático (INECC) para los estudios de ordenamiento ecológico territorial. Los insumos empleados comprenden información climática actual y futura, cubiertas de suelos y propiedades edáficas asociadas al municipio de Gómez Palacio, Durango, México (25.886° N y 103.476° W). Los cálculos realizados a partir de las anomalías para los promedios anuales de precipitación y temperatura indican que el territorio municipal en el escenario A2 podría tener un impacto promedio de 63% causado por la ELV, en tanto que el IA probablemente cambie su promedio histórico de 9.3 a 8.7; se estima que el impacto promedio sobre este índice en el futuro será de  $0.53 \pm 0.2$ .

### ABSTRACT

Modeling the deterioration of natural resources, especially water and soil that results from the global effects of climate change has become a powerful tool in the search for mitigation and adaptation measures. The objectives of this research were: (1) to model the potential impact of climate change for the period 2010-2039, and (2) to offer advice about future risks based on local radiative forcing or critical areas and taking into account two indicators of environmental quality, the aridity index (AI) and laminar wind erosion (LWE).

Evaluation techniques for natural resources, similar to those applied by the Instituto Nacional de Ecología y Cambio Climático (National Institute of Ecology and Climate Change) were used for studies of ecological land use. The inputs include climate information (current and future), soil cover and edaphic properties related to the municipality of Gómez Palacio, Durango, Mexico (25.886° N, 103.476° W). According to calculations estimated from the anomalies for the mean annual rainfall and mean annual temperature, in a future climate change scenario, an average impact of approximately 63% would be caused by LWE, and the AI would change from its historical value of 9.3 to 8.7. It is estimated that the average impact on the AI in the future will be  $0.53 \pm 0.2$ .

**Keywords:** Climate scenarios, modeling, ecological zoning.

## 1. Introduction

In less than a decade, modeling climate processes to assess the deterioration of natural resources has become a powerful tool for determining trends, especially for water and soil (Yu, 2003; Rose, 2005; van Roosmalen *et al.*, 2011). For example, van Roosmalen *et al.* (2011) used a model to determine future changes in the recharge of aquifers in a small (5459 km<sup>2</sup>) hydrological basin in Denmark. They employed a downscaling method with a resolution of 12 km<sup>2</sup> from a regional climatic model (RCM) with a resolution of 40 km<sup>2</sup> identified as HIRHAM4. That model was then nested into the General Climatic Model (GCM) developed by the Hadley Centre.

Recent studies warn about climate changes, particularly alterations in precipitation and temperature variables (Rivera *et al.*, 2007; García-Páez and Cruz-Medina 2009). For example, Magaña *et al.* (2003) and Magaña (2010) argue that under a scenario of global warming, the El Niño/Southern Oscillation (ENSO) cycle could be more frequent and intense, leading to longer drought periods at 25° N latitude, where the state of Durango is located.

These predictions are especially relevant in light of the increasing vulnerability of physical-biotic and socio-economic systems, particularly in the production of staple crops such as maize in Mexico (Monterroso *et al.*, 2011). Therefore, there is an urgent need to develop techniques that not only consider future climatic trends (PNUD, 2005) but also that match the information available to effectively assess the probability of local impacts. Such information can strengthen adaptation measures to climate change (SEMARNAT-INE, 2009).

Consequently, the objectives of this research were:

(1) to model the potential impact of climate change for the period 2010-2039, and (2) to offer advice about future risks based on local radiative forcing or

critical areas and taking into account two indicators of environmental quality, the aridity index (AI) and soil erosion.

## 2. Methodology

### 2.1 Study area, characteristics and location

Gómez Palacio is one of the 39 municipalities of the state of Durango. It has an area of 842.32 km<sup>2</sup>, and it is located (25.886° N, 103.476° W) in a geographical-ecological region known as the Bolsón de Mapimí. This region presents a climate gradient from south to north, ranging from dry (BSohw) to very dry (BWhw). The annual average temperature varies from 20 to 24 °C, and the mean annual rainfall is approximately 200 mm (García, 2003). One of its salient characteristics is that approximately 60% of the territory is used for agriculture with irrigation, as is favored by its topography (slope < 1%); the remaining 40% corresponds to urban and rural (Fig. 1).

### 2.2 Study baseline and indicators of environmental quality (IQA)

The baseline or reference for this study were the conditions of 2010, which serve as a basis for comparison to assess the impact of climate change on a 30-year (2010-2039) time horizon. The environmental characteristics chosen as indicators were the laminar wind erosion (LWE) and AI, the first as the loss of soil due to the wind action on the soil surface, and the second as drought stress. Each is directly correlated with the changes under future scenarios for temperature and rainfall, as described by Magaña *et al.* (2012) for the northeast of Mexico.

### 2.3 IQA modeling and input data

The modeling of the IQA, LWE and AI was developed through two techniques: (1) for the LWE indica-

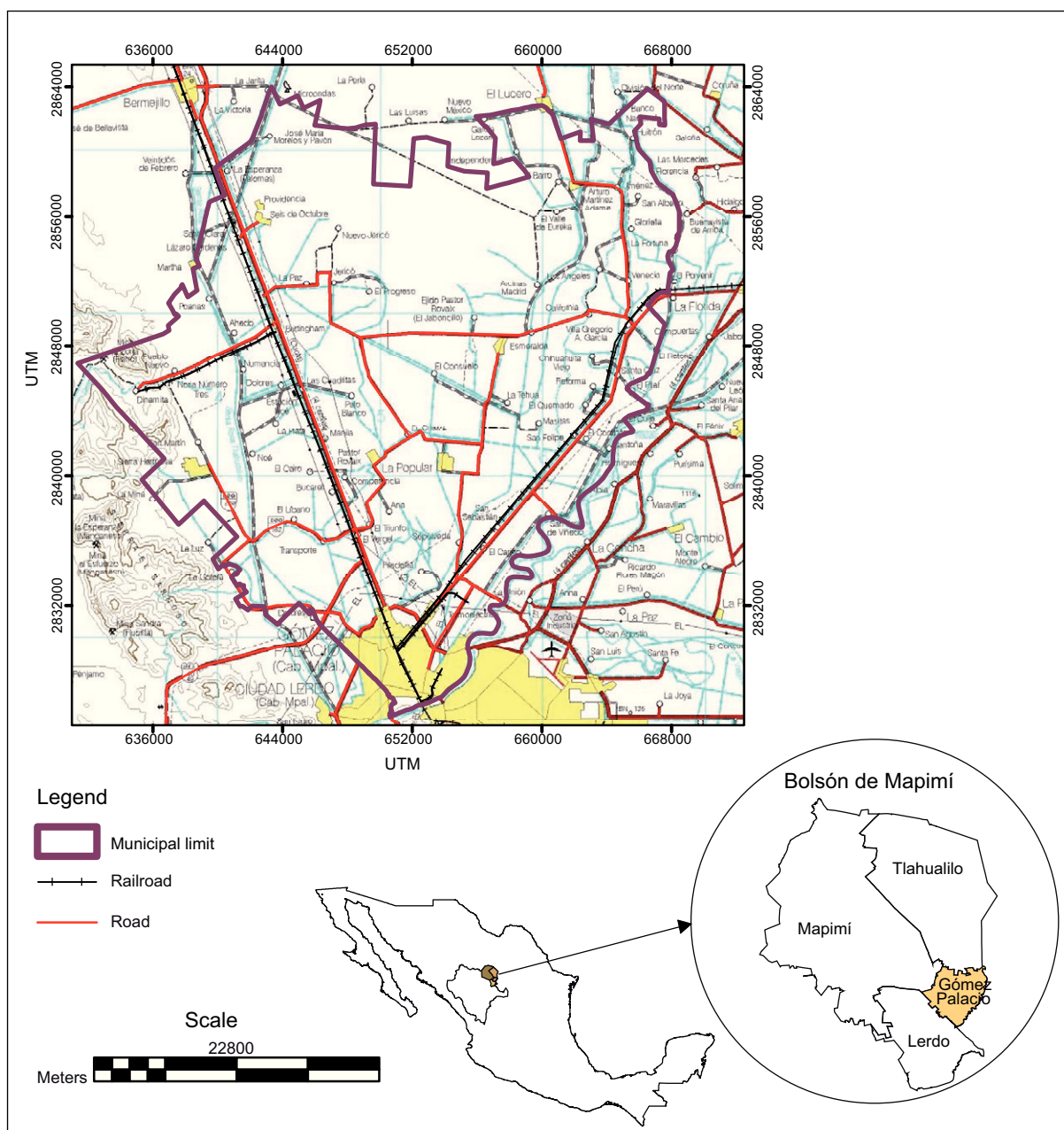


Fig. 1. Geographical location and topographic features of the municipality of Gómez Palacio, Durango, Mexico.

tor, the loss of soil in  $t\ ha^{-1}\ yr^{-1}$  was estimated based on the methodology proposed by INE (1998) for studies of ecological-use zoning, and (2) AI was determined by the De Martonne's aridity index, which has been used by Mercado-Mancera *et al.* (2010) as an estimator of the aridity and desertification in arid land in northwestern Mexico.

The input for the baseline year modeling was the historical data set of weather from the Servicio Meteorológico Nacional (SMN, National Weather

Service), as well as measurements related to the biotic physical environment such as topography, soil and vegetation. Meanwhile, to assess the potential impact on the IQA by future scenarios (2010-2039), projections (metadata) for regional climate change of Mexico were downloaded (INE-SEMARNAT, 2011). These data were generated by downscaling the results of the global circulation models (GCM) used in the Fourth Assessment Report of the IPCC in 2007 (IPCC, 2008).

#### 2.4 Meaning and process for determining LWE

The LWE as an environmental quality index represents the magnitude ( $\text{t ha}^{-1} \text{ yr}^{-1}$ ) of soil loss by wind, which theoretically is incorporated as an additional burden at different heights in the atmosphere. In the lower layer, the air carrying soil has direct effects on human health because it is the layer of air that people breathe. Such impacts can reach many kilometers from where it is produced, affecting both rural and urban areas.

Calculating the baseline LWE (for 2010) began with the determination of the dominant environmental factors in erosion, the action of water or wind. The values depend on indices related to edaphic properties (CATEX, Spanish acronym), use of soil (CAUSO, Spanish acronym), susceptibility of soil to erosion (CAERO, Spanish acronym) and topographical conditions (CATOP, Spanish acronym), which apply according to the predominant process in the erosion.

The basis for the calculation of the erosion rates is in both cases (water or wind) related to the availability of humidity as a result of the presence of rain  $> 10$  mm. Therefore, the mean annual rainfall (MAR) was determined to estimate the rain aggressiveness index (RAI) and wind aggressiveness index (WAI). Both indices depend on MAR, which determines the growth period (GROPE), defined as the number of days per year with availability of water and temperatures conducive to the development of a crop. This GROPE index has been successfully used by Monterroso *et al.* (2011) in a recent study in which they assess the impact of climate change on rain-fed maize in Mexico (Fig. 2).

The first step of this process was to make zoning maps for the RAI and WAI, which were calculated

using digitalization processes (interpolation, reclassification and raster  $\leftrightarrow$  vector) in ArcGis 10 (ESRI) according to the following equations:

$$\text{GROPE} = 0.2408 * (\text{MAR}) - 0.0000372 * (\text{MAR})^2 - 33.1019 \quad (1)$$

$$\text{RAI} = 1.244 * (\text{GROPE}) - 14.7875 \quad (2)$$

$$\text{WAI} = 160.8252 - 0.7660 * (\text{GROPE}) \quad (3)$$

There are three rules for determining the dominant factor in soil erosion: (1) if the value of the RAI is greater than 50 ( $> 50$ ), it is considered a zone of influence for the study of water erosion; (2) if the value of the WAI is greater than 20 ( $> 20$ ), it is considered a zone of influence for the study of wind erosion; and (3) if both factors reach the threshold values, then the magnitude of erosion is calculated separately, or without erosion.

In accordance with these decision rules, the applied analysis (Fig. 2) determined that laminar water erosion is not dominant in the town of Gómez Palacio, so this part of the methodology only describes the procedure to determine the magnitude and distribution of laminar soil erosion by wind. To calculate LWE in  $\text{t ha}^{-1} \text{ yr}^{-1}$ , the following equation was used:

$$\text{LWE} = \text{WAI} * \text{CATEX} * \text{CAUSO} \quad (4)$$

#### 2.5 Aridity index as a drought indicator

De Martonne's AI has been used to characterize climate and indicate drought (Mercado-Mancera *et al.*, 2010). For this study, the following expression was applied:

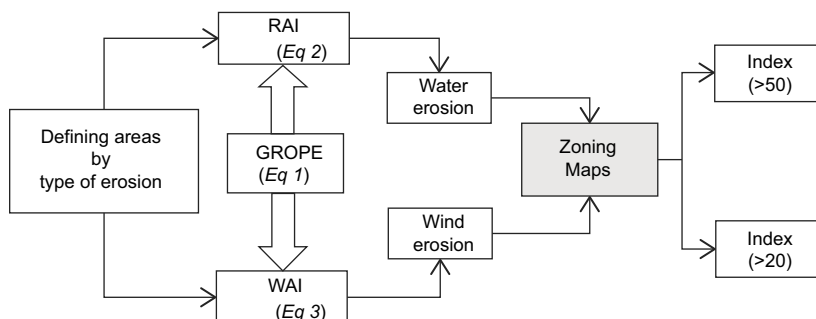


Fig. 2. Flowchart of zoning maps for the generation of aggressiveness indices for rain (RAI) and wind (WAI).

$$AI = \frac{MAR}{10 + MAT} \quad (5)$$

Where AI is the aridity index, which takes dimensionless values between 0 and > 60; MAR is the mean annual rain from historical records and the A2 scenario; MAT is the mean annual temperature from historical records and the A2 scenario; and 10 is a constant value derived from De Martonne’s model (Table I).

Table I. De Martonne’s aridity index.

AI value	Classification
0-5	Desert (hyperarid)
5-10	Semi-desert (arid)
10-20	Semiarid Mediterranean type
20-30	Subhumid
30-60	Wet
> 60	Perwet

Source: [http://www.miliarium.com/prontuario/Medio-Ambiente/Atmosfera/IndicesClima.htm#De\\_Martonne](http://www.miliarium.com/prontuario/Medio-Ambiente/Atmosfera/IndicesClima.htm#De_Martonne).

### 2.6 Origin and management of climate data

Data from 13 weather stations (WS) were used: 12 from the SMN and one from the Instituto Nacional de Investigaciones Forestales Agrícolas y Pecuarias (INIFAP, National Institute for Forestry, Agricultural and Livestock Research), located at the northern region of the municipality. All of them fell within a radius of approximately 65 km. Four WS correspond to the state of Coahuila (WS ID numbers: 5006, 5027, 5028 and 5029) and the other nine to the state of Durango. The metadata for the future scenarios are in this coverage as well (Fig. 3).

### 2.7 Indices related to edaphic properties and land use: CATEX and CAUSO

The estimated values of the indices CATEX and CAUSO for the municipality of Gómez Palacio were created by manipulating the attribute tables of vector data sets containing the CATEX index. The indices were calculated according to matching criteria between the type of soils used in Mexico by INEGI in the cartographic

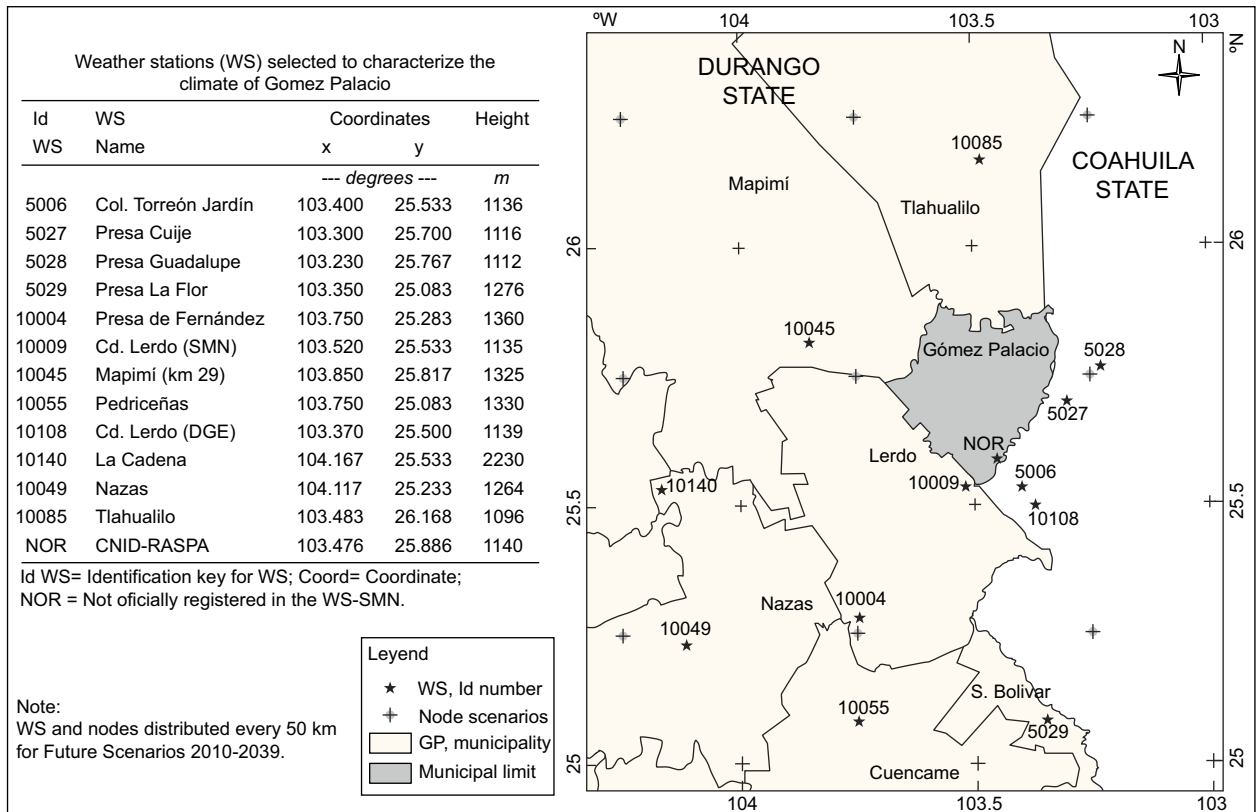


Fig. 3. Integration of selected WS-SMN and their geographical location.

Table II. CATEX and CAUSO indexes.

CATEX	TCPP	C-INEGI, 2007	CAUSO	Category and use
3.5	1	Coarse	0.70	C1, rainfed agriculture
1.75	2	Medium	0.20	C2, irrigated agriculture
1.85	3	Fine	0.15	C3, scrubland
0.87	SPB	PPG	0.30	C4, grassland

TCPP: Textural class and physical phase; SPB: Stony phase or burdensome;  
C-INEGI, 2007: Textural class according to INEGI, 2007.

series I and II. Series I was elaborated based on the soils classification developed by FAO-UNESCO in 1968 and modified by CETENAL in 1970 (Krasilnikov *et al.*, 2013). Series II was based on the World Reference Base for Soils (FAO-ISRIC-ISSS, 1998). The soils of the municipality are almost entirely of calcareous origin, so we selected texture qualification and physical phase. The CAUSO index, associated with the distribution and abundance of vegetation, was estimated based on the identification of four vegetation groups, as well as the land dedicated to agricultural use and under irrigation (Table II).

### 2.8 Metadata for regionalized climate scenarios (2010-2039) to determine the LWE

To assess the climate changes, metadata were downloaded from the SEMARNAT-INE website (<http://zimbra.ine.gob.mx/escenarios/>) corresponding to MAT and MAR for three future scenarios: A2, A1B and B1 for the 2010-2039 period. In the original metadata, each one has a specific format; rain anomalies are in percent, and the temperature is in degrees Celsius (Table III).

The climatic future scenarios produced by Magaña and Caetano (2007), with anomalies for rain and temperature (shown in Table III), are the result of numerous experiments based on the 24 GCM proposed by the IPCC. In fact, this work is the origin of GHG emission lines (IPCC, 2007) whose characteristics are as follows:

*Scenario A1:* Assumes a very rapid global economic growth, up to doubling the world population by mid-century, and the rapid introduction of new and more efficient technologies. It is divided into three groups, which reflect three alternative directions for technological change: intensive fossil fuels (A1FI), non-fossil energy (A1T), and a balance between the various energy sources (A1B).

*Scenario B1:* Describes a convergent world with the same population as A1 but with a more rapid

evolution of economic structures toward a service and information economy.

*Scenario A2:* Describes a very heterogeneous world with strong population growth and both slow economic development and technological change.

### 2.9 Geostatistical analysis and assessing impact

The impact analysis of future climate variability in rainfall and temperature began with the creation of a projected layer (shp), according to the locations ( $x$ ,  $y$ ) of the weather stations. The data were interpolated for each of the variables included in the study ( $z_i$ ), using an inverse distance-weighted (IDW) method in ArcMap 10 (ESRI), the same method used by Karaca (2012). The first product of this process was the creation of a raster layer adjusted to maximum and minimum extreme values. The second product was a change of the properties of the statistical and pixel raster image in tree classes for calculating the changes from historic or current data to the future scenarios. Next, we converted the classified raster image to a vector format, from which it was possible to determine the surface terms most impacted.

## 3. Results and discussion

The WS data set shown above (Table III) was calculated for each variable; for the mean annual rainfall, percent anomalies were subtracted, and for the temperatures, the anomaly value was directly added. The percentage anomalies for both MAR and MAT were very similar among the three future scenarios described by Magaña and Caetano (2007), A2, A1B and B1. Therefore, this single study focused only on local impacts of the A2 scenario.

### 3.1 Analysis of the MAR impact

The values in Table IV, which compares the projected MAR to the historic (HMAR), are consistent with the maximum (287.5 mm) and minimum rainfalls

Table III. HMAR and HMAT and anomalies regionalized for Mexico for three future scenarios of the 2010-2039 period.

WS Id.	WS name	Coordinates		Elevation m	MAR HMAR mm	Anomaly			MAT HMAT	Anomaly		
		Long. W	Lat. N			A2	A1B	B1		A2	A1B	B1
		Degrees				%				°C		
5006	Col. Torreón Jardín	103.4	25.533	1136	256.2	-2.55	-3.08	-2.79	22	0.86	0.926	0.838
5027	Presa Cuije	103.3	25.7	1116	194	-3.32	-3.08	-2.79	21.9	0.86	0.926	0.838
5028	Presa Guadalupe	103.23	25.767	1112	203.3	-3.32	-3.08	-2.79	21.5	0.86	0.926	0.838
5029	Presa La Flor	103.35	25.083	1276	280.3	-2.55	-2.87	-2.94	20.9	0.856	0.929	0.836
10004	Cañón de Fernández	103.75	25.283	1360	320.4	-3.98	-3.94	-3.69	22.1	0.867	0.935	0.835
10009	Cd. Lerdo (SMN)	103.52	25.533	1135	286.6	-2.98	-2.95	-2.24	21	0.851	0.926	0.823
10045	Mapimí (km 29)	103.85	25.817	1325	320.1	-2.98	-2.95	-2.24	19.3	0.851	0.926	0.823
10055	Pedriceñas	103.75	25.083	1330	403.6	-3.98	-3.94	-3.69	19.6	0.867	0.935	0.835
10108	Cd. Lerdo (DGE)	103.37	25.5	1139	270.1	-2.55	-2.87	-2.94	21	0.856	0.929	0.836
10140	La Cadena	104.167	25.533	2230	274.2	-3.76	-2.84	-2.73	21.2	0.865	0.973	0.834
10049	Nazas	104.117	25.233	1264	348.9	-2.81	-2.95	-2.61	20.3	0.883	0.958	0.85
10085	Tlahualilo	103.483	26.168	1096	266.4	-1.64	-2.12	-2.74	20.6	0.861	0.92	0.827
NOR	CENID-RASPA	103.476	25.886	1127	209.6	-3.32	-3.07	-2.78	20.5	0.86	0.926	0.838
			Aver.	1280	279.5	-3.06	-3.06	-2.84	20.9	0.861	0.933	0.835
			Stdev	301	59.46	0.66	0.46	0.44	0.86	0.008	0.015	0.007

WS Id.: Weather station key; Aver.: Average; Stdev: Standard deviation; NOR: Not officially registered in the WS-SMN; HMAR: Historic for mean annual rainfall; HMAT: Historic for mean annual temperature.

Table IV. The relative impact (RI) on MAR in the future scenario A2.

Range	MAR		Impact	
	Historic (HMAR)	Scenario A2 ( $MAR_{ScA2}$ )	ACh ( $HMAR - MAR_{ScA2}$ )	RI %
	mm			
Lower	202.9	196.4	6.5	3.2
Upper	287.5	278.5	9	3.13
Average	245.2	237.4	7.75	3.16

MAR: Mean annual rainfall; ACh: Absolute change; RI%:  $(ACh/HMAR)*100$ .

(202.9 mm) in the 13 WS included in the present study. For the future scenario A2 ( $MAR_{ScA2}$ ), which is given by subtracting the average negative anomalies, the lower limit (196.4 mm) is more affected, with a likely decrease of 6.5 mm per year.

Compared to HMAR, in the  $MAR_{ScA2}$ , the impact of such anomalies on the spatial distribution of the gradient in annual rainfall from west to east (Fig. 4b) is to decrease MAR for both the lower and upper ranges, at 6.5 and 9 mm, respectively, which equals an average impact of 3.16% (Table IV).

To complement the analysis of the changes in MAR from HMAR to 2039 (the A2 scenario), an additional digital process was performed over the “raster” images that represent the distribution of the HMAR with the objective of comparing similar ranges. Data for each time period was reclassified into three categories, and the involved surfaces were calculated (Fig. 4c).

We then compared the historical number of pixels and the surface area in each category to the projected scenario. Pixels from each period were divided into three classes (a1, a2, and a3 for HMAR and b1, b2, and b3 for  $MAR_{ScA2}$ ). The lowest category included lower values in  $MAR_{ScA2}$ . From HMAR to A2, 52% of the surface shifted from class 1 to 2, and between class a3 and b3, the surface lowered 17.73%. In scenario A2, the class with the lowest values for MAR (196.4-237.6) the surface area increased 8.20%, while the surface of the class with the highest values (259.7-278.2) decreased (17.73%), changing from 39 887 to 24 955 ha. It is also important to mention the following:

The average MAR decreased 11.2 mm, to move from 248.5 to 237.3 mm annually between historical values and the future (Fig. 4c).

In the above-mentioned class with the highest values (259.7-278.2), the affected area extends from

the eastern boundary with the municipality of Matamoros, Coahuila, to the north by Tlahualilo, to the western boundary near Arcinas and Pastor Rovaix, and to the north near Lucero and Banco Nacional (Fig. 4b).

There is a concentration of pixels in the lower range in scenario A2 (b3), which magnifies the impact. Although the mean difference between a3 and b3 is 8.9 mm, the impact is much greater because of the number of values concentrated towards the lower limit of that range (Fig. 4d).

Finally, it is important to note the anomalies affecting two WS: Cañon de Fernández (Id. 10004) and Pedriceña (Id. 10055). At these stations, runoff of surface water begins to feed the reservoirs (Francisco Zarco dam), and the agricultural irrigation of Gómez Palacio depends on this runoff. In absolute terms, the MAR could exceed the average for the three scenarios; *i.e.*, the consequence of this declination index is approximately 4%.

### 3.2 Calculation and zoning of the GROPE

The GROPE is an index that was calculated based on Eq. (1), where the independent variable is the MAR. Therefore, it compares anomalies in average annual rainfall in historical and the future scenario A2. We compared HGROPE to  $GROPE_{ScA2}$ . The HGROPE index fell by an average of 7.18% in the future A2 scenario ( $GROPE_{ScA2}$ ). In addition, the boundaries of the ranges change between the historic values (14.2-32.9) and the  $GROPE_{ScA2}$  (12.8-31.1), as shown in Table V.

Based on the relationship that exists between the MAR and GROPE index, we would expect the MAR to be affected to the same extent, although it is not easy to determine the magnitude of the impacts of this signal in the limits of the range considered. To clarify

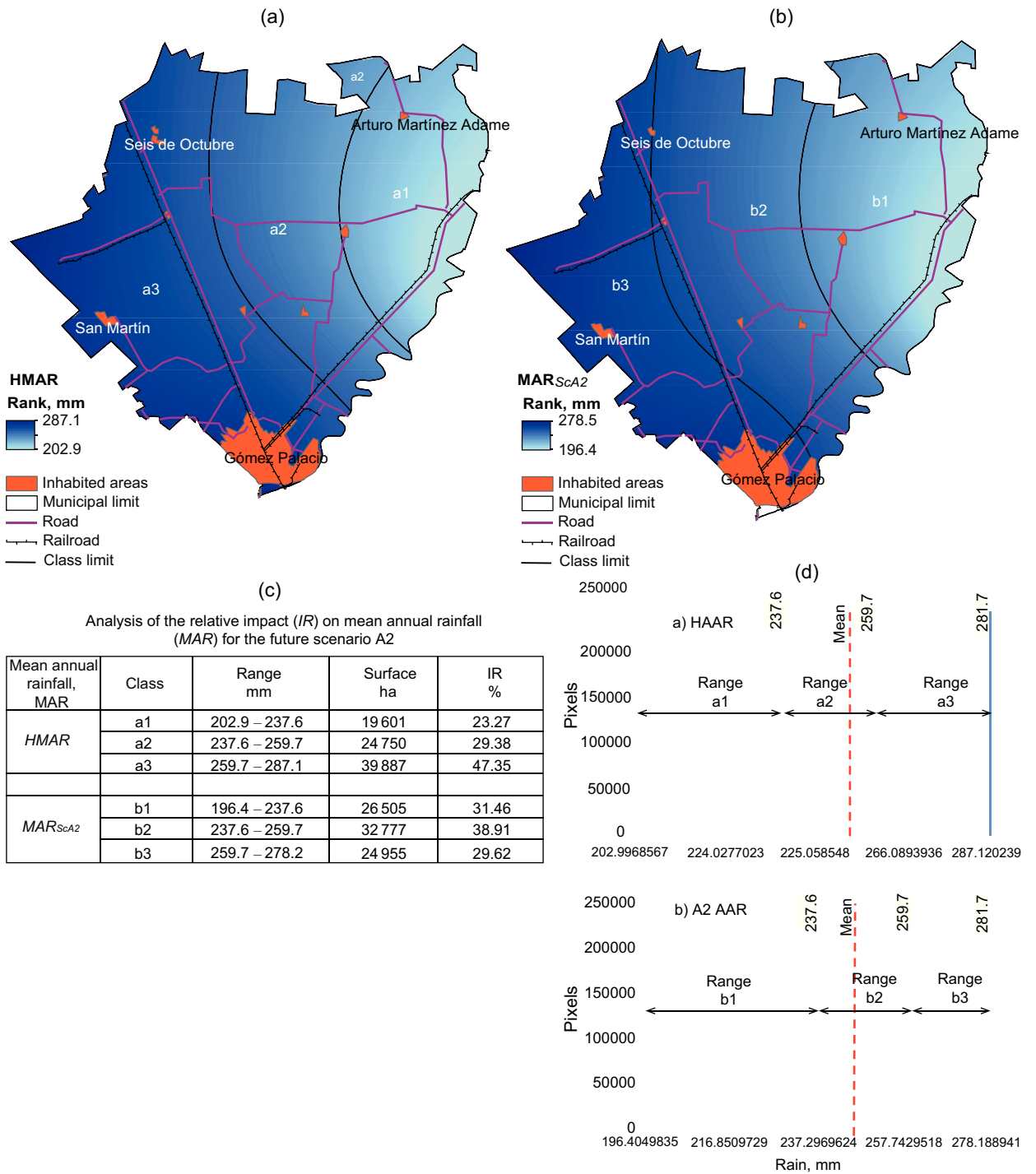


Fig. 4. Spatial distribution of HMAR (a) and MAR<sub>ScA2</sub> (b); impact analysis based on surface and relative impact (c); results of the reclassification of images a and b (d).

Table V. Impact analysis in the GROPE index as a result in the MAR changes.

Range limit	GROPE		Impact	
	Historic HGROPE	Scenario A2 GROPE <sub>ScA2</sub>	ACh (HGROPE - GROPE <sub>ScA2</sub> )	RI%
Lower	14.2	12.7	1.5	10.46
Higher	32.9	31.1	1.8	5.76
Average	23.6	21.9	1.7	7.18

$$RI\% = (ACh/HGROPE)*100.$$

this in terms of the impact at the surface level (Fig. 5) that would be affected, the GROPE index images were also reclassified into three classes (Fig. 5c) and compared.

First, between classes a1 and b1, there is a projected increase of 6937 ha, equivalent to 8.23%, which would imply an extension of 2.7 km from east to west. This extension would occur from Esmeralda, where currently the HGROPE is located, to the west in the vicinity of Pastor Rovaix and Consuelo. Second, between classes a2 and b2, there is a projected increase of 7676 ha, equivalent to 9.11%, which would imply an extension of approximately 5 km from east to west. This extension would occur from La Popular, which is currently HGROPE, to the west near to El Cairo, Estación Noé, La Plata and Bucareli. Third, there is a double impact in the shift between classes a3 and b3. The GROPE index would have a reduction of two units from the HGROPE (26.8-32.9) to the GROPE<sub>ScA2</sub> (26.8-31.1), and the index also has lower maximum values in class b3 (Fig. 5d).

### 3.3 Calculation and zoning of the WAI

As in the previous cases, the WAI could be affected in the future A2 scenario (WAI<sub>ScA2</sub>) because of the way the MAR is affected, although the relationship is more direct for GROPE as described in the methodology (Eq. 1). WAI could therefore be impacted in climate scenario A2 for the territory of Gómez Palacio by an average reduction of 1% and a change in the range of values from historical levels (135.5-149.9) to the A2 scenario (137-151.05), as shown in Table VI.

The spatial distribution of the WAI is presented in Figure 6. One salient change is the growth between classes a2 and b2, which is estimated to affect a total of 33 218 ha, derived from an increase of 10% between HWAI and WAI<sub>ScA2</sub> (Fig. 6c). This increase

includes the area known as Perímetro Lavín, where the following stations are located: El Cairo, Competencia, Noé, Dolores, Numancia and Brittingham (Fig. 6b).

### 3.4 Calculation and zoning of the CAUSO index

The CAUSO is an index defined by current land use (Table II), and the determination of the surfaces that will be occupied by urban nuclei on a horizon of approximately 30 years (2010-2039) was based on the programa de desarrollo urbano (PDU, program of urban development) of the municipality of Gómez Palacio (SEMARNAT, 2012). The distribution of the CAUSO index is shown in Figure 7, where future impacts can be assumed because of the drastic changes in categories C3 and C4. For the first category, there is a probable decrease in scrubland located in the western part of the municipality near Poanas, Dinamita and San Martín. The extent would fall from the 19 793.5 ha (26.9%) currently estimated to 8675.5 ha (12.2%) by 2035. For the second category, there is an estimated increase in the vegetation associated with sandy deserts (Halophyte) in the north of the municipality, which would grow from 4473.1 ha (6.1%) to 15 390.1 ha (21.7%) (Fig. 7c).

### 3.5 Estimation and zoning of the LWE rate

The rate of LWE not only represents the quantity of soil loss per year but is also a way to evaluate environmental loss. To determine the LWE rate, a digital process was conducted based on algebra maps using matrix operations and between digital layers (raster) using Eq. (4). The inputs described above in the context of the A2 scenario were used, as in CAUSO and WAI, with the exception of the edaphic index (CATEX). Edaphic characters such as the texture and the physical phase (stoniness factor) are changes not easily predictable in a short period of time.

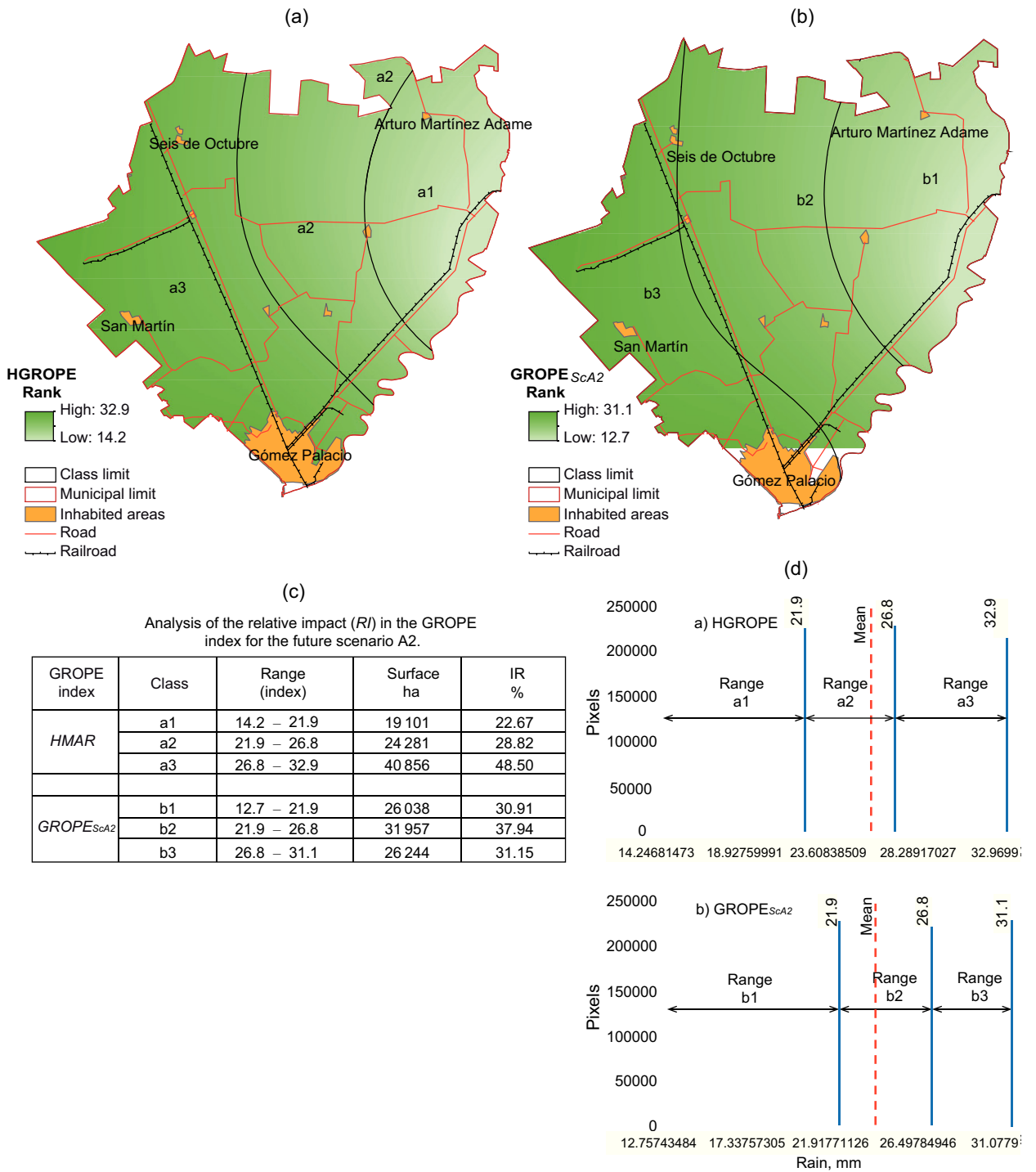


Fig. 5. Spatial distribution of HGROPE (a) and GROPE<sub>ScA2</sub> (b); impact analysis based on surface and relative importance (c); results of the reclassification of images a and b (d).

Table VI. Impact analysis of the WAI as a consequence of the GROPE changes on the municipality of Gómez Palacio.

Range limit	WAI		Impact	
	Historic (HWAI)	Scenario A2 (WAI <sub>ScA2</sub> )	ACh (HWAI – WAI <sub>ScA2</sub> )	RI%
Lower	135.5	137.0	1.50	1.12
Higher	149.9	151.05	1.15	0.77
Average	142.7	144.12	1.42	1.00

$$RI\% = (ACh/HGROPE) * 100.$$

The results indicate an average impact on the order of 63.06%, derived from a change in the range in the historical laminar wind erosion (HLWE) rate from 36-106 to 36-151.4 t ha<sup>-1</sup> yr<sup>-1</sup> in the future for the A2 scenario (LWE<sub>ScA2</sub>), as shown in Figure 8c.

A more detailed analysis of the impact associated with the increased susceptibility of soils to wind erosion and by a lower availability of moisture because of the lower MAR<sub>ScA2</sub> indicates that this effect might be great and could influence nearly one third of the municipality (Fig. 8d). The spatial distribution of the three classes of erosion is shown in Figure 8b.

### 3.6 Analysis of the variables related to the aridity index

In addition to the calculation for LWE, as shown above, the aridity index provides a good complement to determine the magnitude of probable impacts for decreasing MAR and increasing MAT. AI has been examined in the three climate scenarios analyzed for the north and northeast of Mexico (Magaña and Caetano, 2007; Magaña *et al.*, 2012).

### 3.7 Changes in mean annual temperature

According to the climate scenarios in the report of the IPCC (2007), the mean temperature in the northern hemisphere during the second half of the 20th century was likely higher than any other 50 year period in the last 500, and most likely the highest over the past 1300 years.

According to the IPCC report (2007), significant changes were observed in the data for physical (snow, ice and frozen ground; hydrology; and coastal processes) and biological systems (land, marine and freshwater biological systems), and there was great variation in the air surface temperature during the period 1970-2004. The temperature changed on

the order of 1 to 2 °C within 200 km to the north of the Tropic of Cancer (23.5° N). This increase will affect almost all of the municipality, but especially the northern area, where Seis de Octubre and Arturo Martínez Adame are located.

Temperature and rain are obviously fundamental variables in the analysis of the deterioration of natural resources. Both are processed for the historic data set and later were calculated since the anomalies. The results in Table III suggest that the temperature change estimated by HMAT would be from 21 to 21.8 °C in the future A2 scenario (MAT<sub>ScA2</sub>).

### 3.8 Changes in the aridity index

Given the relationship the De Martonne model (Eq. 5) establishes for MAR and MAT, as mentioned above, a decrease of rain will accompany an increase in temperature. In a future scenario there may be environmental deterioration manifested by an increase in aridity and prolonged drought as reported previously for North America and particularly for Mexico (Frederick and Gleick, 2001; UACH-CONAZA-SEDESOL-SAGARPA, 2004; IPCC, 2008).

According to the calculations made from anomalies already described for the MAR and the MAT (Table III), the aridity index in the municipality of Gómez Palacio would change from the historic values (HAI) of 9.3 to 8.7 in the future scenario A2 (AI<sub>ScA2</sub>). It is estimated that the average impact on this index in the future could be  $-0.53 \pm 0.2$  (Table VII).

The estimated impact, in terms of surface area for the AI, indicated that the municipality of Gómez Palacio would most likely become more sensitive due to the tendency toward a hyper-arid condition, and reach index values in the range of 0 to 5, as already specified above (Table I). The impact in this case could cover an area of 13 072 ha, equivalent to the 15.52% of the municipal territory (Fig. 9c).

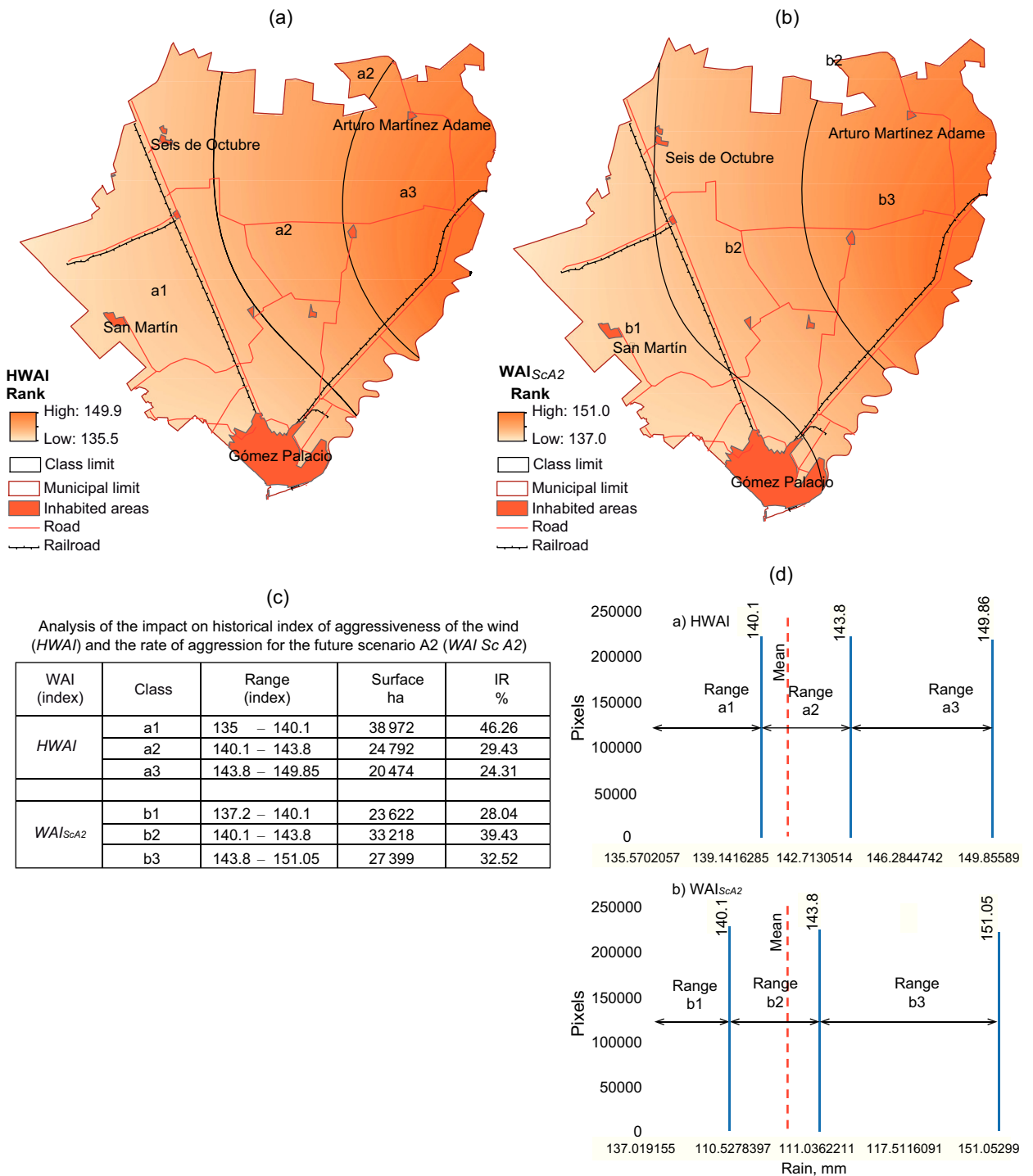


Fig. 6. The spatial distribution of HWAI (a) and WAI<sub>ScA2</sub> (b); analysis of relative impact (RI) based on affected surface (c); results of the reclassification of images a and b (d).

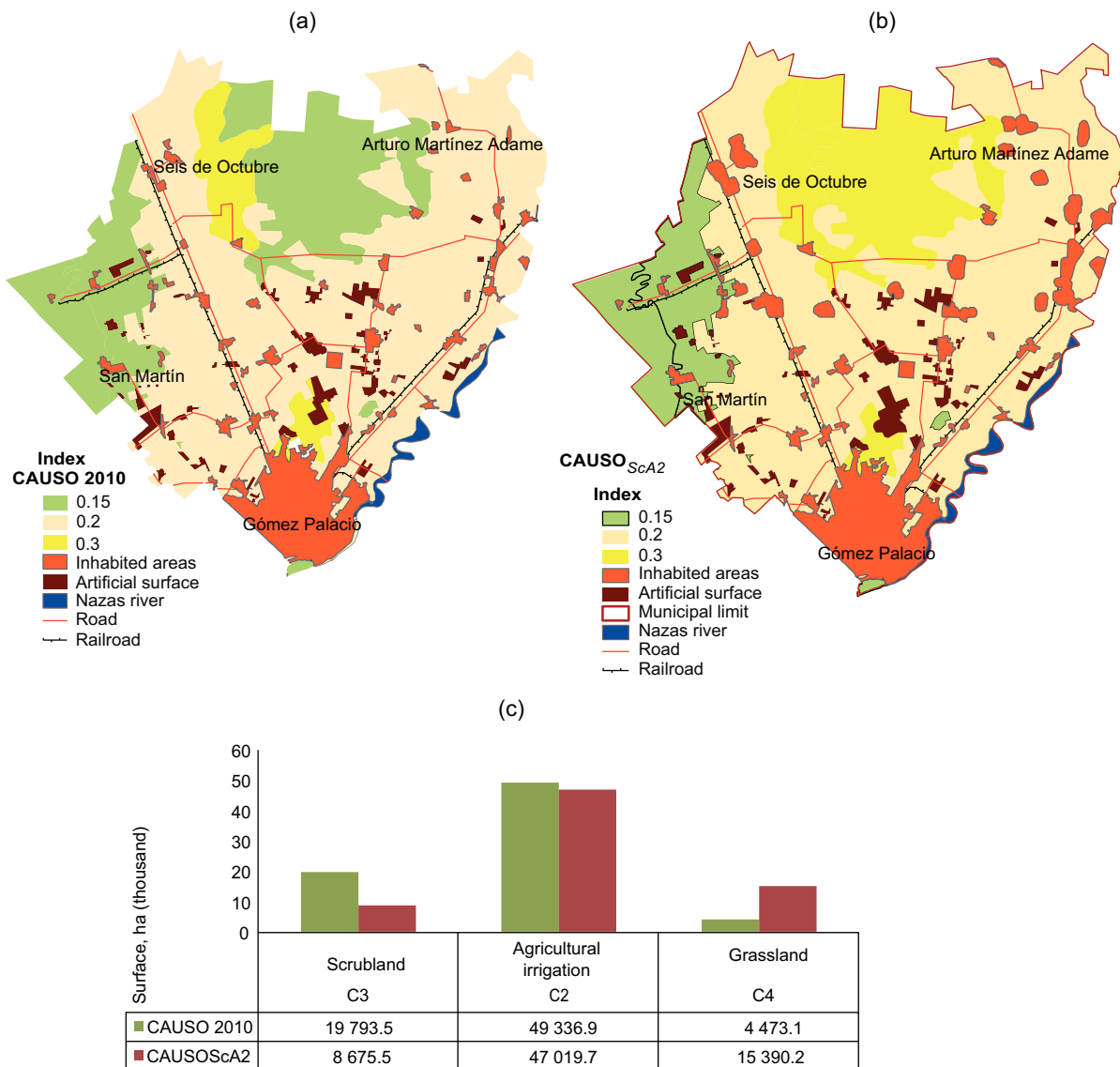


Figure 7. Spatial distribution of CAUSO current (a) and CAUSO<sub>ScA2</sub> (b); impact analysis based on surface and relative importance (c).

It is also important to mention that in addition to the reduction in the range of index values from historical levels (6.5-9.62) to the future scenario AI<sub>ScA2</sub> (6.11-9.17), the average of this index changed from 8.06 to 7.64. Additionally, there is greater aridity in the highest class, as seen in the density of pixels between the two cases (Fig. 9d).

### 3.9 Environmental quality analysis and probable impacts

Environmental quality is a term that relates to certain conditions of “comfort” for people and natural environments or biological systems. The critical elements

are the availability of fresh water, air quality and temperature (Karaca, 2012; Kuo-Jen *et al.*, 2012). The water in the form of rain becomes important in regulating temperature and its relationship with extreme events, such as drought and dust storms, among others (Sun *et al.*, 2003; Batjargal *et al.*, 2006; Zhang *et al.*, 2012).

Arid and semiarid regions will likely experience an increase in temperature and decrease in rain (Rivera *et al.*, 2007; García-Páez and Cruz-Medina, 2009; Magaña *et al.*, 2012), especially for latitudes similar to the Bolsón de Mapimí, the area where Gómez Palacio is located.

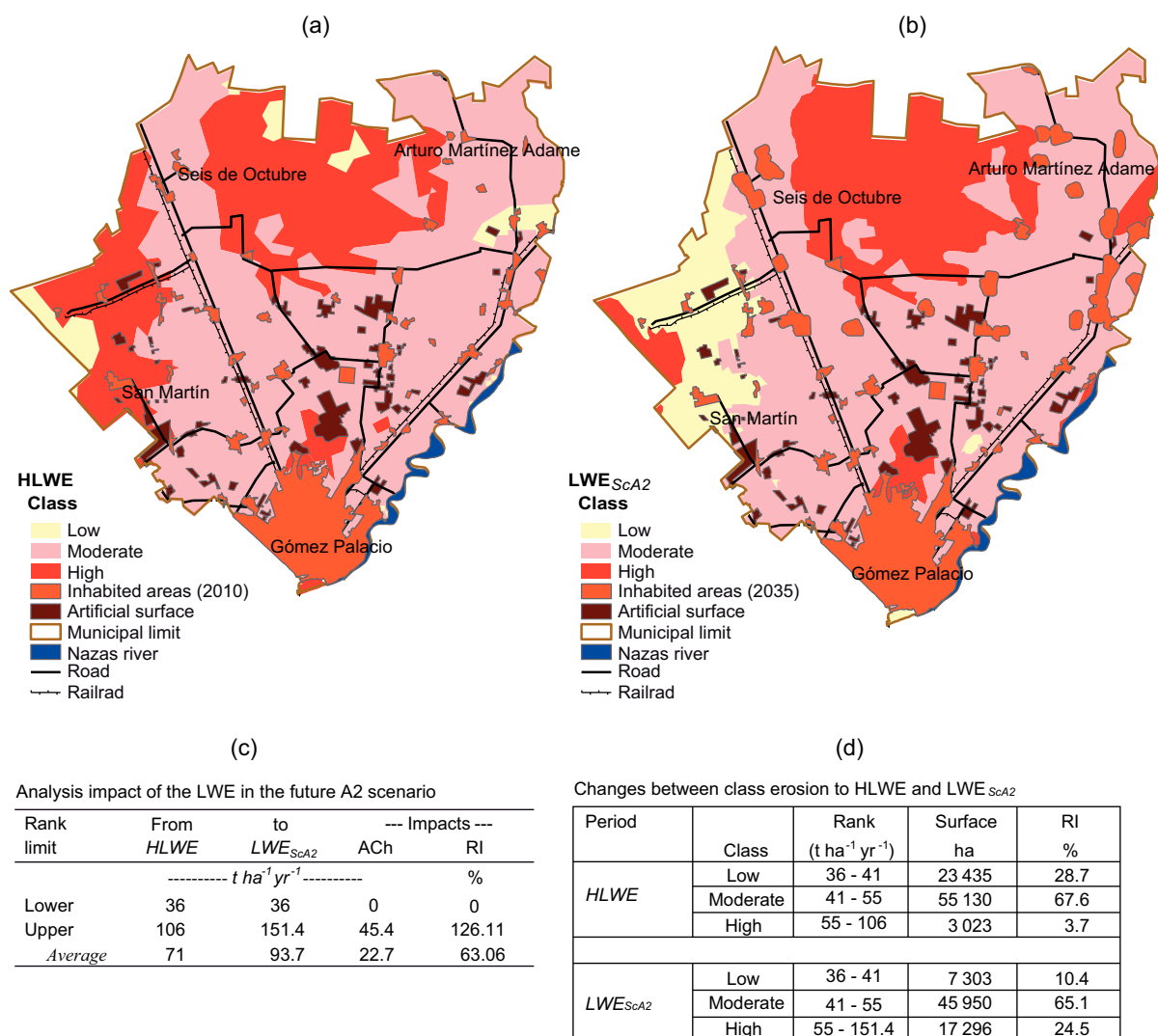


Fig. 8. Spatial distribution of HLWE (a) and LWE<sub>ScA2</sub> (b); impact analysis based on surface and relative importance (c); impact analysis based on surface LWE by ranges and relative classes (d).

Although this study used an average temperature increase of less than  $< 1\text{ }^{\circ}\text{C}$  and a rainfall decline of approximately 3%, the changes may be larger. For example, Magaña *et al.* (2012) remarked that for the north of Mexico in the future A2 scenario, the average temperature towards the end of the 21st century could increase from  $3.5\text{ }^{\circ}\text{C}$  ( $\pm 0.6$ ), with extremes for the drier months (March, April and May) up to  $7\text{ }^{\circ}\text{C}$ , while rainfall could decline by up to 5%.

This decrease in humidity, as shown in Figure 8, could not only negatively impact the rates of soil erosion, with probable losses in the future scenario A2 of up to  $151.4\text{ t ha}^{-1}\text{ yr}^{-1}$ , but could also result in changes in the systems of biological feedback (Breshears *et al.*, 2003; Harper *et al.*, 2010), a crisis

of freshwater availability and negative effects on the air quality due to a drastic increase in suspended particles. This change is potentially harmful to people's health (Razo *et al.*, 2004; Rashki *et al.*, 2011) and could affect the albedo at the level of the surface of the Earth and the atmosphere (Batjargal *et al.*, 2006; Hak-Sung *et al.*, 2011). Figure 10 shows an aerial view of Gómez Palacio municipality and an example of qualitative laminar wind erosion.

The rate of laminar wind erosion was  $151.4\text{ t ha}^{-1}\text{ yr}^{-1}$ , equivalent to the removal and transport of a soil layer between 12.6 and 13.7 mm thick. If the soil is medium textured over the entire area of study, this amount is between  $1100$  and  $1200\text{ kg m}^{-3}$ , which implies a potential loss of approximately 0.4 m in

Table VII. Estimation of changes in the AI from the historic (HAI) to future A2 scenario ( $AI_{ScA2}$ ) in Gómez Palacio.

WS Id.	Name WS-SMN	Coordinates		Aridity Index		
		Long.	Lat.	HAI	$AI_{ScA2}$	ACh
		Degrees		Index		
5006	Col. Torreón Jardín	103.400	25.533	<b>8.0</b>	7.6	0.41
5027	Presa Cuije	103.300	25.700	6.1	5.7	0.36
5028	Presa Guadalupe	103.230	25.767	6.5	6.1	0.38
5029	Presa La Flor	103.350	25.083	9.1	8.6	0.47
10004	Cañón de Fernández	103.750	25.283	10.0	9.3	0.65
10009	Cd. Lerdo (SMN)	103.520	25.533	9.2	8.7	0.52
10045	Mapimí (km 29)	103.850	25.817	10.9	10.3	0.62
10055	Pedriceña	103.750	25.083	13.6	12.7	0.91
10108	Cd. Lerdo (DGE)	103.370	25.500	8.7	8.3	0.45
10140	La Cadena	104.167	25.533	8.8	8.2	0.56
10049	Nazas	104.117	25.233	11.5	10.9	0.64
10085	Tlahualilo	103.483	26.168	8.7	8.3	0.38
NOR	CENID-RASPA	103.476	25.886	6.9	6.5	0.4
			Aver.	9.3	8.7	0.53
			Stddev	2.1	2.0	0.20

ACh: Absolute change on aridity index ( $HAI - AI_{ScA2}$ ); the value of the historic temperature (bold) for the WS-SMN 5006 was averaged using the values from the nearest neighborhood; Aver.: Average; Stddev: Standard deviation; NOR: Not officially registered in the WS-SMN.

30 years. For this type of soil, these values exceed the rates of soil loss tolerance ( $5-12 \text{ t ha}^{-1} \text{ yr}^{-1}$ ) proposed by the United States Department of Agriculture (USDA) (Montgomery, 2007).

An example of changes in the biological feedback is that the removal of the soil directly affects the role of nitrogen (N). N determines plant productivity, and in arid environments, the soil frequently presents large accumulations of calcium carbonate that push the soil pH to a range of 7 to 8. At this pH, phosphorus (P) is in complex forms and not available (Munson *et al.*, 2011; Schlesinger *et al.*, 2011), a set of conditions that matches the selection criteria of the parameters for the CATEX index that was described in the methodology. In response to a deficiency of N and P, *Larrea tridentata* shows the highest levels of efficient use of nutrients that have been found in woody plants.

#### 4. Conclusions

The models for the LWE and the AI suggest that in the immediate future (2010-2039) the climatic conditions of the area of study and its surroundings will deteriorate and could lead to a steady decline of environmental quality and health. There are two

important implications of this study. First, the models can serve to warn people of the risks to human and natural environments from extreme conditions such as droughts and dust storms. Secondly, it is possible to identify local changes in use of the soil and deforestation.

Finally, it is important to mention that the magnitude and distribution of the impact on the territory are relevant to planning the management of natural resources. This research should be taken into account in decision-making about preventing impacts on natural resources now and in the future.

#### Acknowledgements

This article is part of the results of the research carried out within the framework of the Programa Estatal de Acciones ante el Cambio Climático (State Program of Action on Climate Change) Durango (PEACC-DGO) and Aguascalientes (PEACC-AGS) during a post-doctoral stay conducted between 2011 and 2012. Thanks to Joaquín Pinto Espinoza and Adriana Martínez Prado, both responsible for the PEACC-DGO, and Elsa Marcela Ramírez López, head of PEACC-AGS.

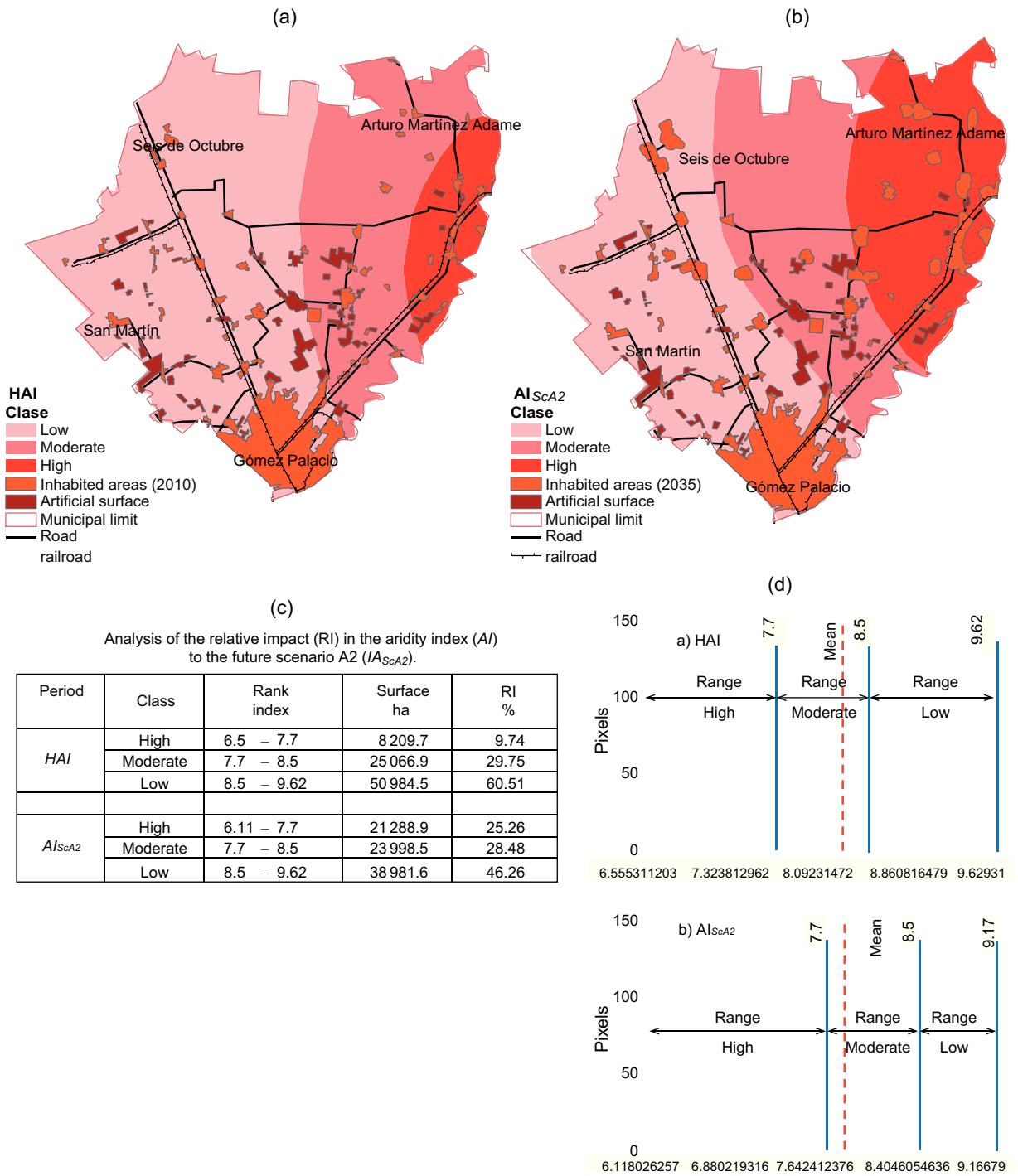


Fig. 9. Spatial distribution of HAI (a) and AI<sub>ScA2</sub> (b); impact analysis based on surface and relative importance (c); impact analysis based on surface AI by ranges and relative classes (d).



Fig. 10. Current aerial view at different scales of the superficial area of Gómez Palacio and a close-up to the high critical zone of laminar wind erosion.

## References

- Batjargal Z., J. Dulam and Y. S. Chung, 2006. Dust storms are an indication of an unhealthy environment in East Asia. *Environ. Monit. Assess.* **114**, 447-460, doi:10.1007/s10661-006-5032-3.
- Breshears D. D., J. J. Whicker, M. P. Johansen and J. E. Pinder, 2003. Wind and water erosion and transport in semi-arid shrub land, grassland and forest ecosystems: Quantifying dominance of horizontal wind-driven transport. *Earth Surf. Proc. Land.* **28**, 1189-1209, doi:10.1002/esp.1034.
- FAO-ISRIC-ISSS, 1998. World reference base for soil resources. World Soil Resources Reports 84. Food and Agriculture Organization of the United Nations, Rome. Available at: <http://www.fao.org/docrep/W8594E/W8594E00.htm>.
- Frederick K. D. and P. H. Gleick, 2001. Potential impacts on US water resources. In: *Climate change, science strategy and solutions* (E. Claussen, V. Arroyo Cochran and D. P. Davis, Eds.). The Pow Center on Global Climate Change. Brill, Boston, pp. 63-82.
- García E., 2003. Distribución de la precipitación en la República Mexicana. *Investigaciones Geográficas* **50**, 67-76.
- García-Páez F. and I. R. Cruz-Medina, 2009. Variabilidad de la precipitación pluvial en la región Pacífico norte de México. *Agrociencia* **43**, 1-9.
- Hak-Sung K., C. Yong-Seung and L. Sun-Gu, 2011. Characteristics of aerosol types during large-scale transport of air pollution over the Yellow Sea region and at Cheongwon, Korea, in 2008. *Environ. Monit. Assess.* **184**, 1973-1984, doi:10.1007/s10661-011-2092-9.
- Harper R. J., R. J. Gilkes, M. J. Hill and D. J. Carter, 2010. Wind erosion and soil carbon dynamics in south-western Australia. *Aeolian Research* **1**, 129-141, doi:10.1016/j.aeolia.2009.10.003.
- INE, 1998. *Ordenamiento ecológico del territorio. Memoria técnica y metodológica*. Instituto Nacional de Ecología, Secretaría de Desarrollo Social, México, 66 pp.
- IPCC, 2007. *Climate change 2007: Impacts, adaptation and vulnerability. Contribution of Working Group II*

- to the Fourth Assessment Report of the Intergovernmental Panel on Climate Change (M. L. Parry, O. F. Canziani, J. P. Palutikof, P. J. van der Linden and C. E. Hanson, Eds.). Cambridge University Press, Cambridge, 976 pp.
- IPCC, 2007. *Cambio climático 2007: Informe de síntesis. Contribución de los grupos de trabajo I, II y III al Cuarto Informe de Evaluación del Grupo Intergubernamental de Expertos sobre el Cambio Climático* (R. K. Pachauri and A. Reisinger, Eds.). IPCC, Geneva, 104 pp.
- Karaca F., 2012. Determination of air quality zones in Turkey. *JAPCA J. Air Waste Ma.* **62**, 408-419, doi:10.1080/10473289.2012.655883.
- Krasilnikov P., M. C. Gutiérrez-Castorena, R. J. Ahrens, C. O. Cruz-Gaistardo, S. Sedov and E. Solleiro-Rebolledo, 2013. *The soils of Mexico*. World Soils Book Series. Springer, 175 pp., doi:10.1007/978-94-007-5660-1\_2.
- Kuo-Jen L., P. Amar, E. Tagaris and A. G. Russell, 2012. Development of risk-based air quality management strategies under impacts of climate change. *JAPCA J. Air Waste Ma.* **62**, 557-565, doi:10.1080/10962247.2012.662928.
- Magaña V. O., J. L. Vázquez, J. L. Pérez and J. B. Pérez, 2003. Impact of El Niño on precipitation in Mexico. *Geof. Int.* **42**, 313-330.
- Magaña V. O. and E. Caetano, 2007. Pronóstico climático estacional regionalizado para la República Mexicana como elemento para la reducción de riesgo, para la identificación de opciones de adaptación al cambio climático y para la alimentación del sistema: cambio climático por estado y por sector (informe final). Dirección General de Investigación sobre Cambio Climático, SEMARNAT-INE. 41 pp.
- Magaña V. O., 2010. *Guía para generar y aplicar escenarios probabilísticos regionales de cambio climático en la toma de decisiones*. Centro de Ciencias de la Atmósfera, Universidad Nacional Autónoma de México, 80 pp.
- Magaña V. O., D. Zermeño and C. Neri, 2012. Climate change scenarios and potential impacts on water availability in northern Mexico. *Clim. Res.* **51**, 171-184, doi:10.3354/CR01080.
- Mercado-Mancera G., E. Troyo-Diéguez, A. Aguirre-Gómez, B. Murillo-Amador, L. F. Beltrán-Morales and J. L. García-Hernández, 2010. Calibración y aplicación del índice de aridez de De Martonne para el análisis del déficit hídrico como estimador de la aridez y desertificación en zonas áridas. *Universidad y Ciencia* **26**, 51-64.
- Monterroso A. I., A. C. Conde, D. Rosales, J. D. Gómez and C. Gay, 2011. Assessing current and potential rain-fed maize suitability under climate change scenarios in Mexico. *Atmósfera* **24**, 53-67.
- Montgomery D. R., 2007. Soil erosion and agricultural sustainability. *P. Natl. Acad. Sci. USA* **104**, 13268-13272.
- Munson S. M., J. Belnap and G. S. Okinb, 2011. Responses of wind erosion to climate-induced vegetation changes on the Colorado Plateau. *P. Natl. Acad. Sci. USA* **108**, 3854-3859.
- PNUD, 2005. *Marco de políticas de adaptación al cambio climático: desarrollo de estrategias, políticas y medidas* (B. Lim and E. Spanger-Siegfried, Eds.). Programa de las Naciones Unidas para el Desarrollo, New York, 274 pp.
- Rashki A., C. J. Rautenbach, P. G. Eriksson, D. G. Kasakoutis and P. Gupta, 2011. Temporal changes of particulate concentration in the ambient air over the city of Zahedan, Iran. *Air Quality, Atmosphere & Health*, doi:10.1007/s11869-011-0152-5.
- Razo I., L. Carrizales, J. Castro, F. Díaz-Barriga and M. Monroy, 2004. Arsenic and heavy metal pollution of soil, water and sediments in a semi-arid climate mining area in Mexico. *Water Air Soil Poll.* **152**, 129-152, doi:10.1023/B:WATE.0000015350.14520.c1.
- Rivera del Río R., G. Crespo Pichardo, R. Arteaga Ramírez and A. Quevedo Nolasco, 2007. Comportamiento espacio temporal de la sequía en el estado de Durango, México. *Terra Latinoamericana* **25**, 383-392.
- Rose C. W., 2005. Erosion by water, modeling. In: *Encyclopaedia of Soil Science* (R. Lal, Ed.). Marcel Decker, New York, pp. 468-472.
- Schlesinger W. H., J. J. Cole, A. C. Finzi and E. A. Holland, 2011. Introduction to coupled biogeochemical cycles. *Front. Ecol. Environ.* **9**, 5-8.
- SEMARNAT, 2012. *Estudio técnico para el ordenamiento ecológico y territorial del municipio de Gómez Palacio, Durango. Resumen ejecutivo*. Secretaría de Medio Ambiente y Recursos Naturales, Secretaría de Recursos Naturales y Medio Ambiente de Durango, México, 265 pp. Available at: [http://www.gomezpalacio.gob.mx/2010-2013/images/stories/ecologia/consulta/Resumen\\_Ejecutivo\\_Gomez\\_palacio.pdf](http://www.gomezpalacio.gob.mx/2010-2013/images/stories/ecologia/consulta/Resumen_Ejecutivo_Gomez_palacio.pdf) [last accessed on March 5, 2013].
- SEMARNAT-INE, 2009. *México, cuarta comunicación nacional ante la Convención Marco de las Naciones Unidas sobre Cambio Climático*. Secretaría de Medio Ambiente y Recursos Naturales, Instituto Nacional de Ecología, México, 274 pp. Available at: <http://www.>

- semarnat.gob.mx/informacionambiental/documents/sniarn/pdf/Cuarta\_Comunicacion\_Nacional.pdf.
- SEMARNAT-INE, 2011. Sistema de información de escenarios de cambio climático regionalizados (SIECCRe). Metadatos y mapas para SIG. Available at: <http://zimbra.ine.gob.mx/escenarios/> [last accessed on September 24, 2011].
- Sun L., X. Zhou, J. Lu, Y-P, Kim and Y-Seung Chung. 2003, Climatology, trend analysis and prediction of sandstorms and their associated dust fall in China. *Water Air Soil Poll.* **3**. 41-50.
- UACH-CONAZA, 2004. *Escenarios climatológicos de la República Mexicana ante el cambio climático*. Universidad Autónoma Chapingo, Comisión Nacional de Zonas Áridas, México, 169 pp.
- Van Roosmalen L., T. O. Sonnenborg, K. H. Jensen and J. H. Christensen, 2011. Comparison of hydrological simulations of climate change using perturbation of observations and distribution-based scaling. *Vadose Zone J.* **10**,136-150, doi:10.2136/vzj2010.0112.
- Yu B., 2003. A unified framework for water erosion and deposition equations. *Soil. Sci. Soc. Am. J.* **67**, 251-257.
- Zhang Q., J. Li, V. P. Singh, C. Y. Xu and Y. Bai, 2012. Changing structure of the precipitation process during 1960-2005 in Xinjiang, China. *Theor. Appl. Climatol.* **110**, 229-244, doi:10.1007/s00704-012-0611-4.